Nonstoichiometry and Defect Chemistry in Praseodymium-Cerium Oxide

TODD S. STEFANIK & HARRY L TULLER

Massachusetts Institute of Technology, Department of Materials Science and Engineering, Crystal Physics and Electroceramics Laboratory, Cambridge, MA 02139, USA

Abstract. Praseodymium cerium oxide ($Pr_xCe_{1-x}O_{2-\delta}$) is a mixed ionic-electronic conductor with high levels of nonstoichiometry under oxidizing conditions resulting from reduction of Pr^{4+} to Pr^{3+}. Coulometric titration measurements performed on ($Pr_xCe_{1-x}O_{2-\delta}$) with $x = 0.2$ are generally consistent with those derived from electrical conductivity measurements. Nevertheless, a somewhat larger degree of nonstoichiometry measured via coulometric titration implies that non-charged defect species may be significant in the system.

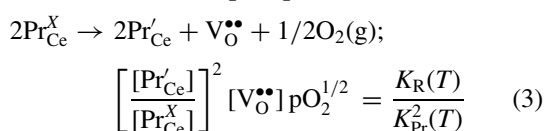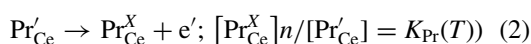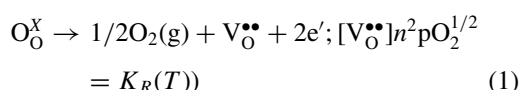**Keywords:** electrical conductivity, coulometric titration, defect modeling

Introduction

Cerium oxide has long been studied for use as a solid oxide ion electrolyte [1]. Trivalent or divalent dopants are typically added to the system to create oxygen vacancies and suppress electron conductivity under reducing conditions [2]. The focus of this study is praseodymium doped cerium oxide ($Pr_xCe_{1-x}O_{2-\delta}$), in which Pr is capable of changing valence between Pr^{3+} and Pr^{4+} at relatively high oxygen pressures. The relatively high ion conductivity, electronic hopping conductivity, and large nonstoichiometry observed in the system make it appealing as a potential fuel cell electrode material, surface-effect gas sensor, or mass-sensitive gas sensing material [3].

In previous work, we have shown that the praseodymium-cerium oxide (PCO) system exhibits a pO_2-dependent ionic conductivity at high pO_2's and, in high Pr content materials, impurity band conductivity at high pO_2's. A defect model capable of describing total conductivity in the system has been developed, based on the interpretation of the experimentally determined pO_2 and Pr dependence of the electrical conductivity [3]. Reduction of the CeO_2 host lattice via the formation of oxygen vacancies and quasi-free electrons is described Eq. (1). Pr forms deep levels within

the CeO_2 band gap and the ionization of Pr^{3+} to Pr^{4+} by excitation of the electron into the conduction band is described by Eq. (2). The existence of deep empty traps (i.e. Pr^{4+}) at high pO_2 lowers the energy for reduction and leads to an increase in the overall nonstoichiometry of the system as described in Eq. ((3). The defect model assumes a pO_2-independent vacancy mobility (such that all changes in oxygen ion conductivity arise due to changes in the vacancy concentration fixed by the concentration of Pr^{3+}). While this assumption is likely not valid, particularly at high doping levels, the majority of electrical conductivity is electronic in nature at the high pO_2 values examined during coulometric titration studies. Only an electronic impurity band conductivity can account for the maximum observed in conductivity at high pO_2 values. Since the dominant conductivty fitted at high pO_2 is electronic in nature, errors that may be introduced due to variable vacancy mobility are not expected to be significant in the range of interest in this study. The effects of temperature variation, pO_2 variation, and geometric factor errors have been analyzed and found to be insignificant relative to the magnitudes of conductivity measured. A detailed discussion of these analyses is beyond the scope of this publication and will be presented at a later date. While electrical conductivity, by its very nature, can only account for charged mobile defects, coulometric titration

can be used, as in this study, to measure directly the extent of nonstoichiometry and thereby establish the contribution of neutral defects to the defect equilibria in PCO. The reaction constant for the ionization of Pr^{3+} to Pr^{4+}, $K_{Pr}(T)$, is determined via numerical fitting of both conductivity and titration data and the results of the two methods are compared to one another and show good agreement at sufficiently high temperatures. Evidence suggesting the existence of uncharged oxygen species is discussed.

$$O_O^X \rightarrow 1/2 O_2(g) + V_O^{\bullet\bullet} + 2e'; [V_O^{\bullet\bullet}]n^2 pO_2^{1/2}$$
$$= K_R(T)) \tag{1}$$

$$Pr'_{Ce} \rightarrow Pr_{Ce}^X + e'; \left[Pr_{Ce}^X\right]n/[Pr'_{Ce}] = K_{Pr}(T)) \tag{2}$$

$$2Pr_{Ce}^X \rightarrow 2Pr'_{Ce} + V_O^{\bullet\bullet} + 1/2 O_2(g);$$

$$\left[\frac{[Pr'_{Ce}]}{[Pr_{Ce}^X]}\right]^2 [V_O^{\bullet\bullet}] pO_2^{1/2} = \frac{K_R(T)}{K_{Pr}^2(T)} \tag{3}$$

Experimental

Powders were produced using a chemical co-precipitation route to ensure complete cation mixing. Mixtures of $Ce(NO_3)_3$ and $Pr(NO_3)_3$ were mixed in the appropriate mole ratio, diluted to a concentration of 1 M and dripped into an excess of 0.5 M oxalic acid. The resulting metal oxalate precipitates were washed three times in distilled water, then dried and calcined at 700°C for 1 hour. If evidence of incomplete decomposition was observed (via XRD), the calcining step was repeated. The ultimate particle size obtained from X-ray peak broadening measurements and BET surface analysis was approximately 20 nm, though SEM micrographs indicate that the powder was highly agglomerated.

Electrical conductivity samples were made by iso-pressing the powders to approximately 275 MPa and firing at 1425°C for 10 hours. The density of the resulting samples was greater than 90% theoretical density for all samples, though the density of heavily doped samples was less than that of samples containing less praseodymium. Rectangular bar shaped samples were cut from the resulting pellets and four electrical contacts were painted onto each sample using platinum ink. Platinum wires were wrapped around these electrodes and more paint was applied to ensure good electrical contact. Six samples were places in a pO_2 controlled furnace and measured simultaneously. Oxygen pressure was controlled using Ar/O_2 mixtures for high pO_2 and CO/CO_2 mixtures for low pO_2. Intermediate pO_2 values were obtained by electrochemically pumping oxygen into a flowing stream of 1000 ppm CO in CO_2, thereby increasing the otherwise low pO_2 of the buffer system. The pO_2 values reported were measured using a zirconia sensor in close proximity to the sample. Samples were allowed to equilibrate at a given pO_2 and temperature until the resistance of the sample varied only within the noise of the measurement. An I-V sweep was then collected and the slope of this curve was used to obtain the reported conductivity values.

Nonstoichiometry was determined by coulometric titration using a method similar to that of Schneider and coworkers [4]. Electrodes were applied to the inner and outer surface of a small YSZ crucible. A known mass of sample powder was sealed into the crucible with a YSZ lid using a glass seal at 1000°C. The titration cells were then cooled to room temperature and moved to another furnace for measurements. The Pt electrodes were shorted to allow the flow of oxygen through the YSZ. Once equilibrium between the inside and outside of the cell had been achieved, oxygen was electrochemically pumped through the YSZ crucible by applying a fixed current to the Pt electrodes. Integration of the total current over time and an appropriate correction for the "dead volume" of the sample cell yielded, by application of Faraday's law, the total amount of oxygen removed from the sample powder. A second set of Pt electrodes (applied to the YSZ lid) were used to measure the open circuit Nernst emf and thereby the oxygen pressure in the titration cell. Together, the two measurements yielded oxygen nonstoichiometry as a function of pO_2. During pumping, the total voltage on the titration cell was limited to 0.9 V to ensure that the YSZ was not electrochemically reduced. The quality of the glass seal was tested by sealing an empty titration cell (no sample), removing oxygen to a very low pO_2 ($<10^{20}$ atm), and watching the leakage over time. At 700°C, 10^{10} atm pO_2 was held for two days. The leak rate was lower at lower temperatures. Such low leak rates should not influence the results of these experiments as 10^{-5} atm pO_2 was the minimum pO_2 achieved during titration of cells with specimens inside of them. While data was collected for 1, 5, and 20% Pr samples, only the 20% Pr data will be discussed here.
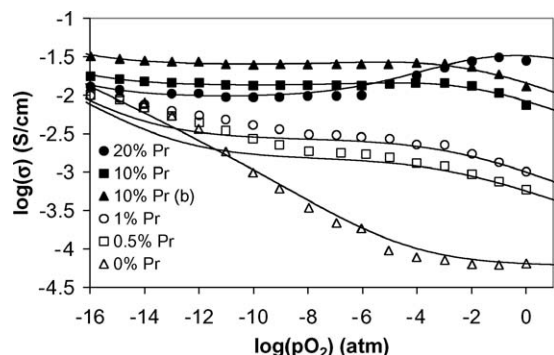
Fig. 1. Total conductivity in PCO at 700°C as a function of pO$_2$. Solid lines represent fits based on the proposed defect model (see text).

Results and Discussion

The total conductivity as a function of pO$_2$ at 700°C for samples of PCO ranging from 0–20% Pr is shown in Fig. 1. At low pO$_2$'s, the behavior is similar to that expected from CeO$_2$ doped with fixed valence acceptors. Under highly reducing conditions, reduction of the host Ce^{4+} results in the generation of free electrons and increasing electron conductivity. Increasing acceptor concentration (in this case, Pr^{3+}) results in an increase in oxygen vacancy concentration and a corresponding increase in the ion conductivity in the pO$_2$-independent plateau region. A maximum ionic conductivity is observed for 10% PCO, followed by a decrease in conductivity resulting presumably from defect association at higher doping levels (indicative of a concentration dependent ionic mobility). For doped samples with Pr levels below 20%, a decrease in conductivity is observed at high pO$_2$ due to, as we demonstrate below, re-oxidation of Pr^{3+} to Pr^{4+} and corresponding decrease in oxygen vacancy concentration. At sufficiently high Pr doping levels (clearly evident for 20% Pr), an increase in conductivity with increasing pO$_2$ is assigned to the formation of an impurity band in which electron/hole hopping can occur. At low Pr concentration, the individual Pr dopant atoms are isolated and conduction must occur within the valence or conduction band. As concentration is increased, however, the discreet dopant energy levels begin to overlap and form an impurity band in which polaron hopping may occur. The complete defect model is described elsewhere [3]. The solid lines in Fig. 1 represent the best fits based on the proposed defect model.
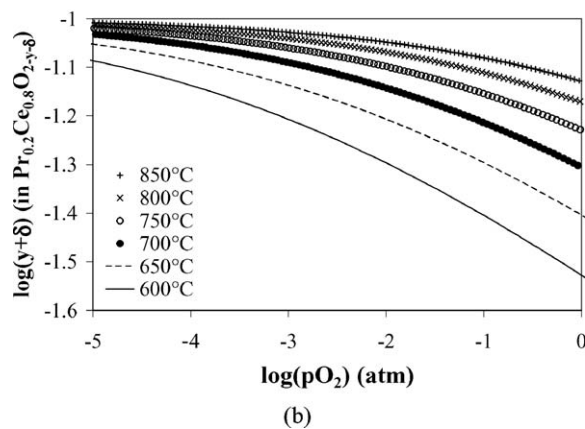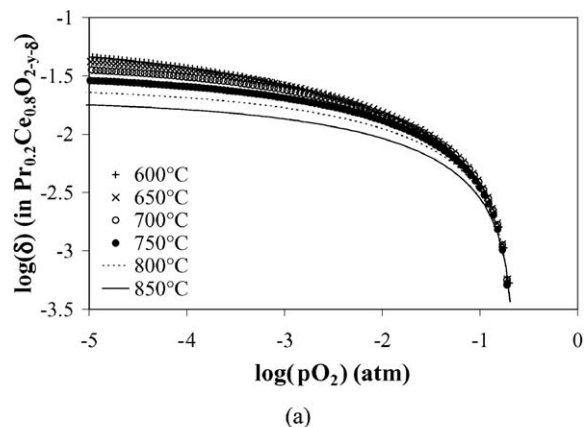

(a)

(b)

Fig. 2. Calculated nonstoichiometry in 20% PCO as a function of oxygen pressure and temperature. (a) shows the change in nonstoichiometry (δ) from the reference nonstoichiometry in air (y), while (b) shows the total nonstoichiometry in the sample ($y + \delta$).

Based on the concentration of oxygen vacancies predicted by the defect model, the anticipated nonstoichiometry data could be calculated. Two plots of nonstoichiometry are shown in Fig. 2. Figure 2(a) shows a plot identical to experimental data collected during a typical coulometric titration experiment. Air is used as a reference, and the plotted results actually correspond to the change in stoichiometry from the nonstoichiometry of the sample in air. As seen in Fig. 2(a), this raw data can be rather convoluted and no obvious trends appear when the data is simply plotted as collected. Figure 3(b) shows the total nonstoichiometry in the system, including the initial nonstoichiometry in air (the reference state for the experiment) and the expected trend of higher overall nonstoichiometry at higher temperature is observed.
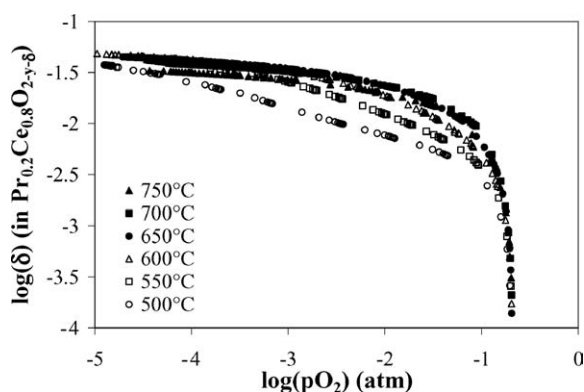
Fig. 3. Change in nonstoichiometry in 20% PCO relative to the initial nonstoichiometry at atmospheric oxygen pressure (*y*).

Fig. 4. Total nonstoichiometry in 20% PCO, including *y*, the fitted initial nonstoichiometry in air (the reference state for the experiment).

Fig. 5. Arrhenius plots of the Pr reduction constant (K_{Pr}) in $Pr_{0.2}Ce_{0.8}O_{2-y-\delta}$ obtained via electrical conductivity and coulometric titration experiments.

The nonstoichiometry in 20% PCO at several temperatures is shown in Fig. 2. As demonstrated in Fig. 2, no trends in the magnitude of the data as a function of temperature should be expected, however, the character of the individual temperature curves is worth noting. At temperatures of 600°C or higher, the nonstoichiometry curves are smooth, and uniform and appear to saturate at low pO_2. At 500 and 550°C, nonstoichiometry as a function of pO_2 yields a segmented curve with flat portions, and at 500°C, the data never appears to saturate. It is likely that polarization of the titration cell and the very long pumping times required at these relatively low temperatures (many hours per decade of pO_2 collected) introduce errors into the measurements. Regardless of the source, the non-characteristic shape of the response observed at 500 and 550°C lowers confidence in the data at those temperatures.

The coulometric titration data were fitted to the defect model previously developed from the electrical conductivity data. The cerium reduction constant was assumed to be identical to that obtained from electrical conductivity fitting. The praseodymium ionization constant and the initial nonstoichiometry in the system at 0.21 atm pO_2 (y) were fitted using a minimization of the square of the error between the fit and experimental values. Initial values of the fitting parameters were taken from the best fits of the electrical conductivity data. Figure 4 shows the total nonstoichiometry in 20% PCO, including the best fit of the initial nonstoichiometry (y) in the system. The fits are quite good at large nonstoichiometry. There is some discrepancy at high pO_2's, but overall the fits describe the experimental results quite well.
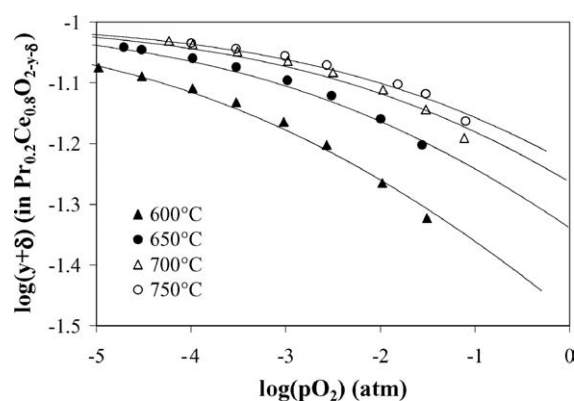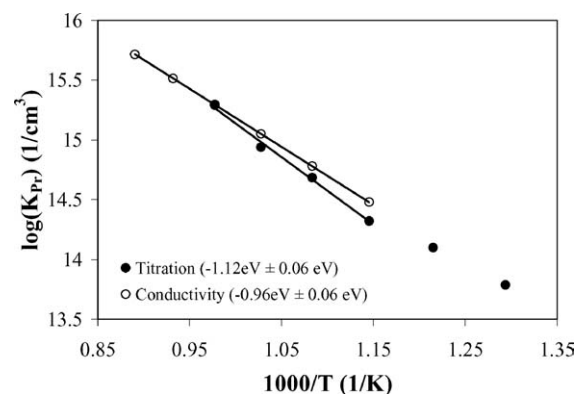
The Arrhenius plots of the K_{Pr} in 20% PCO obtained via electrical conductivity and via coulometric titration data are compared in Fig. 5. The two different methods yield similar results at temperatures of 600°C or higher (where confidence in the titration data is highest). The Pr ionization energies of approximately 1 eV indicate that Pr doping creates a deep trap 1 eV below the conduction band of CeO_2. If all else is held constant, Eq. (3) indicates that the total nonstoichiometry in the system (the total oxygen vacancy concentration) is proportional to $K_{Pr}^{2/3}$, meaning that a lower K_{Pr} value is indicative of higher overall nonstoichiometry. It can be seen that the overall nonstoichiometry measured using coulometric titration is somewhat higher than that measured by electrical conductivity experiments. While this does not offer conclusive evidence, it at least points to the possibility that non-charged oxygen species may

exist in PCO. This would not be surprising, given the high levels of nonstoichiometry attainable in the PCO system.

Summary

Coulometric titration experiments were performed on the PCO system in order to independently verify the degree of nonstoichiometry under controlled temperature and pO_2 predicted by a defect model derived from an analysis of electrical conductivity measurements and to look for evidence of non-charged defect species. While the praseodymium reduction constants derived from the two experimental techniques were largely consistent with one another, a somewhat larger degree of nonstoichiometry measured via coulometric titration implies that non-charged defect species may indeed be significant in the PCO system.

Acknowledgments

References

1. H.L. Tuller and A.S. Nowick, *Journal of the Electrochemical Society,* **122**, 255 (1975).
2. M. Mogensen, N.M. Sammes, and G.A. Tompsett, *Solid State Ionics,* **129**, 63 (2000).
3. T.S. Stefanik and H.L. Tuller, in *Materials Research Society Symposium Proceedings: Solid State Ionics—2002,* edited by P. Knauth, J.-M. Tarascon, E. Traversa, and H.L. Tuller (Materials Research Society, Warrendale, PA, 2002), vol. 756, p. 163.
4. D. Schneider, M. Godickemeier, and L.J. Gauckler, *Journal of Electroceramics,* **1**, 165 (1997).